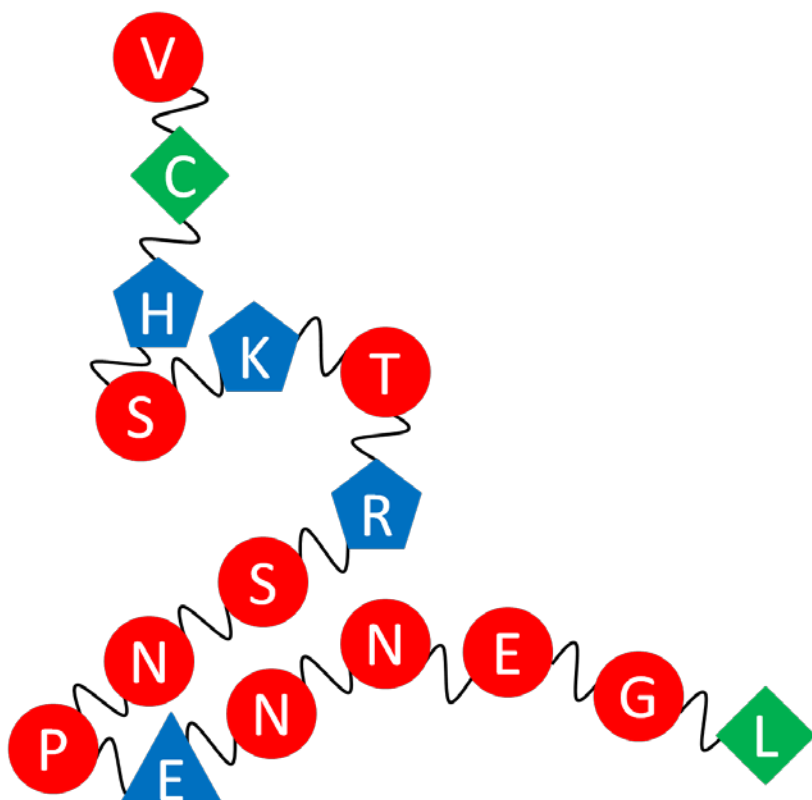


CHALMERS



Membrane Interaction of the Antisecretory Peptide AF16

Master of Science Thesis in the Master Degree Programme Applied Physics

CHUN MAN

Department of Chemical and Biological Engineering

Division of Physical Chemistry

CHALMERS UNIVERSITY OF TECHNOLOGY

Gothenburg, Sweden, 2013

Membrane Interaction of the Antisecretory Peptide AF16

CHUN MAN, swedenchunman@gmail.com

© CHUN MAN, 2013

Department of Chemical and Biological Engineering
Chalmers University of Technology
SE-412 96 Gothenburg
Sweden
Telephone + 46 (0) 31-772 1000

Examiner: Bengt Nordén

Supervisor: Maria Matson Dzebo

Cover:

The amino acids serise of AF16: circles, polar, uncharged; pentagons, polar, positively charged; triangles, polar, negatively charged; diamond, hydrophobic. The structure does not corrspond to the real structure.

Abstract

Antisecretory peptide AF16 is a potential drug for curing fatal diseases with hypersecretion of body fluids, e.g. diarrhea, or inflammation. However, the mechanism behind the peptide's curing effect is not understood, a knowledge needed for developing it into a drug. In this thesis, studies on AF16 were carried out on a molecular level, focusing on the membrane-peptide interaction using negatively charged liposomes. Linear dichroism was applied to study the binding geometry of AF16. Though the binding geometry was not confirmed, significant binding of AF16 and modified versions of the peptide to membrane was observed. Fluorescence spectrum of tryptophan labeled AF16 was used for estimating the binding affinity of AF16. It was found that the peptide is more likely to bind to membrane at pH 5, however, the binding is weak at both pH 5 and pH 7.4. The binding affinity was also studied by isothermal titration calorimetry but no conclusion can be drawn due to the weak signal. It was, however, concluded that the peptide is aggregating in concentration of 0.5 mM. To confirm that no pores are induced upon membrane binding of AF16, ANTS/DPX assay was employed and no ANTS leakage was observed.

Contents

Abstract.....	2
Introduction.....	4
Theory.....	5
Biological Membranes.....	5
Liposomes.....	5
Peptides.....	5
Antisecretory factor (AF) and the peptide AF16.....	6
Fluorescence Spectroscopy.....	6
Tryptophan Emission.....	7
ANTS/DPX Leakage Assay.....	7
Isothermal Titration Calorimetry (ITC).....	8
Linear Dichroism (LD) Spectroscopy.....	9
Circular Dichroism (CD) Spectroscopy.....	10
Dynamic Light Scattering (DLS).....	11
Material and Methods.....	11
Material.....	11
Preparation of Large Unilamellar Vesicles (LUV).....	11
Isothermal Titration Calorimetry (ITC).....	11
ANTS/DPX Leakage Assay.....	12
Linear Dichroism (LD) Spectroscopy.....	12
Circular Dichroism (CD) Spectroscopy.....	13
Dynamic Light Scattering (DLS).....	13
Fluorescence Spectroscopy.....	13
Results and Discussion.....	13
Isothermal Titration Calorimetry (ITC).....	13
Dynamic Light Scattering (DLS).....	16
Circular Dichroism (CD) Spectroscopy.....	17
ANTS/DPX Leakage Assay.....	17
Linear Dichroism (LD) Spectroscopy.....	19
Fluorescence Spectroscopy.....	20

Concluding Remarks.....	24
Future Aspect.....	24
Acknowledgement.....	24
References	25

Introduction

The rapid growth of medical technology has made many diseases become curable. However, there is still no effective therapy for many fatal illnesses. For instance, diarrhea causes 1.5 million children’s deaths each year [1]. Therefore, development of new effective drugs is necessary, where antisecretory peptide AF16 could be a solution.

Antisecretory Factor (AF), also named S5a and Rpn10, is a protein which modulates secretion in the intestine [2]. It caught the attention of medical scientists because studies show that animals exposed to the bacteria *Escherichia coli* have higher AF level compared with animals which were not exposed. The first purification of AF was done in 1986 [3] and its amino acid sequence was identified in 1995 [4]. Two years later, the active site of AF was found to be eight amino acids located between position 35 and 42 in the amino acid sequence [5]. Some peptides were derived from AF. For example, AF16 is a peptide consisting of 16 amino acids [6]. In its sequence, the first 7 amino acids correspond to the active site of AF and the rest are for stabilization.

More recently, studies have proved that the level of plasma AF in human does affect body condition. It has been shown that AF cures diseases where secretion and inflammation is important part of the condition [7, 8]. Since the success of curing patents by increasing the AF level in plasma [9-13], AF16 was proposed as a drug. The performance of AF16 has been assessed on animals to cure diarrhea induced by cholera toxin [14] and increased intracranial pressure (ICP) [6] with positive results. However, the underlying mechanism must be understood before AF16 can be developed into a drug.

The first step of peptide-cell interaction is membrane association. In this master thesis, studies on AF16 were carried out on a molecular level, focusing on the membrane-peptide interaction by using a lipid membrane model called liposome. In order to compare the membrane affinity of AF16 in different conditions, isothermal titration calorimetry (ITC) and fluorescence spectroscopy were used. The binding was also further studied with linear dichroism (LD) for insights in the binding geometry and a leakage assay was used to confirm that binding does not cause membrane pores. Circular dichroism (CD) and dynamic light scattering (DLS) were used to identify the structure of AF16.

Theory

Biological Membranes

The cell membrane defines the boundary of a cell and the first step of all peptide-cell interaction is membrane association. The membrane is mainly composed by lipids and proteins. Lipid consists of a hydrophilic head group and two hydrophobic tails and self-assembles into bilayers in aqueous solution, with the head groups facing the solution and tails in the interior [15]. This structure restricts large or charged molecules to transport across the membrane. Proteins and gangliosides insert in or lay on the membrane surface. The charge on the membrane varies in different position, but it is usually negatively charged since 10-20% of lipids are anionic.

Liposomes

Since the cell membrane is very complex, it is not suitable for studying a specific property. Hence, membrane models are developed to simplify the study. One of the most commonly used membrane models is liposomes, which are classified in size and lamellarity. Large unilamellar vesicle (LUV) (Figure 1) is one type of liposomes. It is a vesicle composed of a single bilayer of lipids, with 100 nm diameter. The surface charge is controlled by mixing different ratio of lipids. In this thesis, three types of lipid were used. They are DOPC, a zwitterionic lipid, DOPG, an anionic lipid, and DSPE-mPEG2000, an anionic lipid with peg-coated head group avoid to liposome aggregation by steric hindrance.



Figure 1 LUV is a vesicle composed of a bilayer of lipids.

Peptides

Peptides are short sequences (2-50) of amino acids linked by peptide bonds, which are covalent bonds formed by the elimination of a water molecule from carboxyl group in one amino acid and amino group in another. One end of peptide is an amino group, which is referred as the beginning of the peptide (N terminus), and the other end is a carboxyl group (C terminus). There are more than 20 different amino acids which are classified as non-polar, uncharged polar, acidic and basic, and hence the structure and chemical properties of each peptide depends on its amino acid sequence. The amino sequence is the primary structure of peptides and many peptides form secondary structures, usually α -helices or β -sheets, by hydrogen bonding. Peptides are chiral molecules and all natural peptides are

left-handed [15]. The function of peptide depends on its active site, which can be the whole peptide or only a part of it. Therefore, peptide or protein with same active site shares equal function.

Antisecretory factor (AF) and the peptide AF16

AF is a 41 kDa protein [4] which can cure some secretion or inflammation related diseases [7, 8]. Clinical studies were carried out by orally taking in of specially processed cereals (SPC) or AF containing food to increase the plasma AF level [9, 10]. Increasing the level of AF in plasma has been shown to be a possible treatment for patients with inflammatory bowel disease (IBD), ulcerative colitis (UC), Crohn's disease, Ménière's disease or diarrhea [9-13].

The sequence responsible for the antisecretory effect has been identified and a number of peptides were developed. AF16 is the shortest peptide containing the active site of AF and its sequence is VCHSKTRSNPENNVGL [5] and its molecular mass is 1754.95 gmol⁻¹. The first 7 amino acids correspond to the active site of AF and the rest are for stabilization. Since AF16 and AF share the same active site, AF16 is a possible drug. Cell and organism studies on animals have shown that AF16 counteracts intestinal hypersecretion by blocking the permeation of anions of cell membrane which could affect the generation of action potentials in nerve cells controlling the water and ion transport system [16]. However further studies must be done to fully understand the mechanism of AF16.

The amino acids in AF16 are varied in their properties and there are 4 positions where deprotonation can occur. At pH 5, the net charge is +2 while it becomes +1 at pH 7.4. Therefore, it is expected that AF16 is more likely to bind to negatively charged membrane at pH 5 if the binding is of electrostatic character. Since AF16 does not absorb or fluoresce, tryptophan labeled AF16 was also used in this study to be able to use spectroscopic methods. Peptides were labeled either at the N-terminus or the C-terminus and are referred to WAF16 or AF16W.

Fluorescence Spectroscopy

Fluorescence is the phenomenon when a substance adsorbs and becomes excited by electromagnetic radiation of a given wavelength and then emits light with another wavelength. Usually, the emitted photon has higher wavelength than the adsorbed photon, hence the emitted photon is red shifted.

A simple case of fluorescence is illustrated in Figure 2. An electron in ground state S_0 is excited by a high energy photon and transfers to excitation state S_1 (blue arrow). Since the relaxation time of vibration relaxation is shorter, the electron releases some of its energy through vibration relaxation (black arrow) to lower state in S_1 . The electron returns to ground state S_0 by emitting a lower energy photon (red arrow).

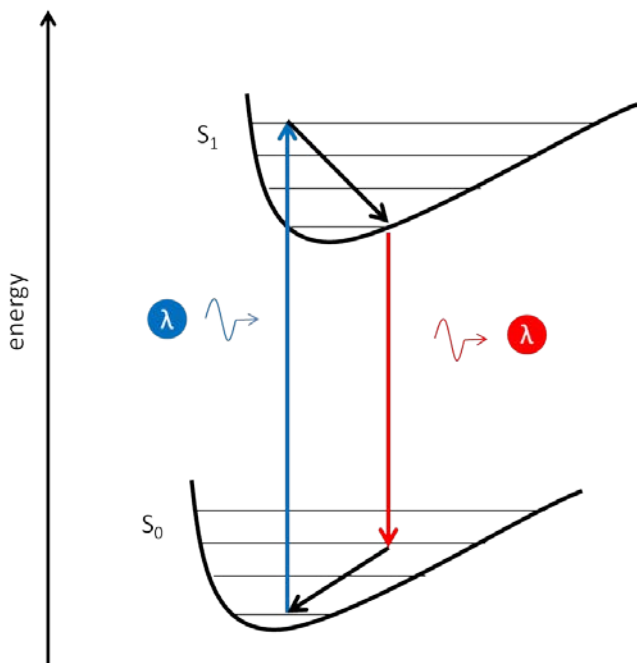


Figure 2 The principle of fluorescence. A blue photon is absorbed and this is followed of the emission of a photon with a red shifted wavelength.

However, in reality it is much complicated. There is unlimited number of vibrational state in each excitation state hence the excitation spectrum and emission spectrum are continues spectra with a distribution of wavelengths rather than emission of a single wavelength. The energy states can be affected by the environment resulting in a shifted spectrum and a change in quantum yield, defined as the ratio of the number of photons emitted to the number of photons absorbed. The fluorescence can also be affected by the presence of a quencher, then energy release due to electron transfer from excited state to ground state is absorbed by quencher rather than emitted as a photon [17].

Tryptophan Emission

Tryptophan is a fluorescence amino acid. The emission spectrum of tryptophan is sensitive to the local environment [18]. In a polar environment (e.g. aqueous solution), the emission is red shifted compared to in a non-polar environment (e.g. bound to lipid membrane). Therefore, by titrating peptide containing tryptophan with a liposome solution, emission spectra in different peptide to lipid ratios $[P]:[L]$ can be recorded and hence binding of peptide can be quantified [19-21].

ANTS/DPX Leakage Assay

To investigate whether AF-16 is inducing pore formation in lipid membranes upon binding, ANTS/DPX assay was used for determining aqueous content leakage [22-25]. ANTS is fluorescent dye and DPX is its quencher and their structure are shown in Figure 4. Liposomes are formed in a buffer solution containing ANTS and DPX. Before the leakage

experiment, the liposomes are passed through a column, eluted with buffer with no ANTS and DPX. As ANTS and DPX are in high concentration inside the vesicle, the fluorescence intensity of ANTS is low due to quenching by DPX. If pores are induced by the peptide interacting with the vesicle membrane, ANTS and DPX can leak out from liposomes and be diluted into the buffer resulting in an increased fluorescence which can be detected by fluorescence spectroscopy.

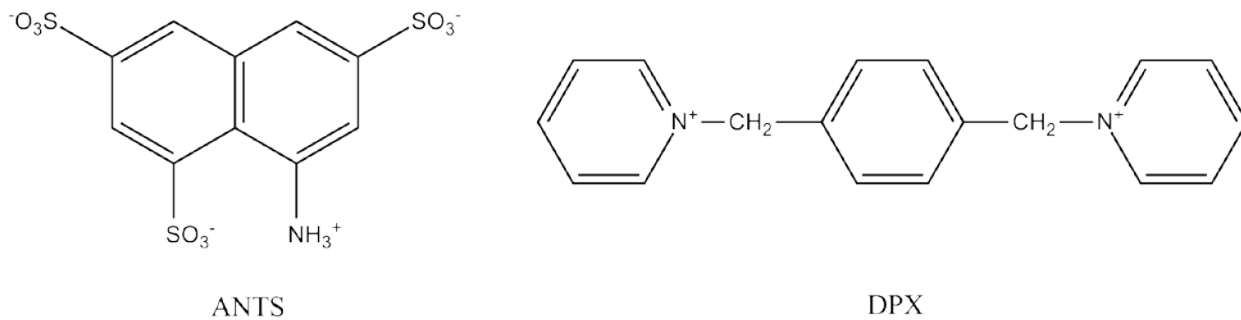


Figure 3 Structures of the fluorescent dye ANTS and its quencher DPX.

Isothermal Titration Calorimetry (ITC)

Isothermal titration calorimetry (ITC) was used to study the membrane affinity of AF16, this is done by measuring the released or absorbed heat upon the interaction. The ITC is composed by several components (Figure 3). A reaction cell, surrounded by a water bath, is loaded with a solution containing one of the molecules of interest. An injection syringe is filled with a solution of another compound, which then is titrated into the reaction cell under stirring. The temperature inside the reaction cell is regulated to be same as the reference cell by a heat sink which is connected only through thermopiles. The voltage output of thermopiles is proportional thermo power flow into the reaction cell from the heat sink. Therefore, the heat being released or absorbed in each titration is measured [26]. The raw data output of the ITC measurement is the rate of the heat flow into the reaction cell against time. After the i^{th} injection, a peak is produced in the data set and its area corresponds to the heat q_i released or absorbed in the reaction cell. This value is related to the binding enthalpy ΔH .

$$q_i = v\Delta H\Delta L_i \quad (1)$$

v is the volume of reaction cell and ΔL_i is the increase in the concentration of bound ligand after the i^{th} injection. Negative peaks are obtained for an exothermic process while, for an endothermic process, the peaks are positive. Usually, the area of the peaks becomes smaller after each injection until the binding is saturated. The remaining small peaks are due to the dilution of reactant and mechanical effects [27]. The heat released in each step q_i is then plotted against the molar ratio $[P]:[L]$ of titrating solution and the data is then fitted with a suitable binding model and the binding constant can be determined.

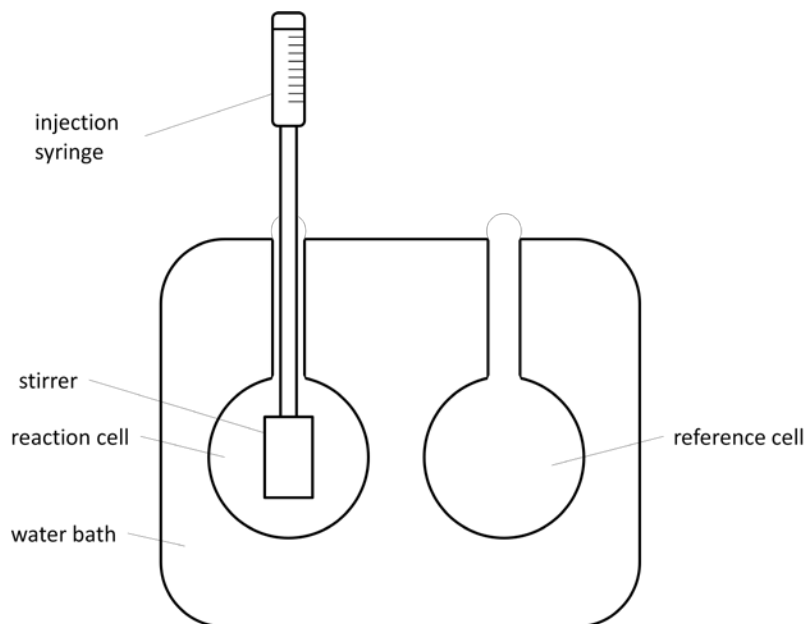


Figure 4 The core components of ITC. Liposomes were loaded in the reaction cell surrounded by a water bath. AF16 solution was loaded in injection syringe and titrated into the reaction cell. Stirrer was equipped for mixing. The temperature difference between reaction cell and reference cell was measured and controlled with a heat sink, connected with thermopiles.

Linear Dichroism (LD) Spectroscopy

To study the binding geometry of AF16 on membrane, Linear Dichroism (LD), which is defined as the difference in absorption of light linearly polarized parallel and perpendicular to an orientation axis (Equation (2)) [28], was measured.

$$LD = A_{\parallel} - A_{\perp} \quad (2)$$

LD can only be measured for samples which are oriented. For instance, a coquette cell shown in Figure 5, can be used to orient samples. The coquette cell is constructed by two cylinders with a gap between them. The outer cylinder rotates during measurement whereas the inner is kept static. The sample is filled in the gap between two cylinders. Liposomes subjected to a shear flow deforms to a cylinder like structure capped by two hemispheres, hence a macroscopic orientation axis is gained [29, 30].

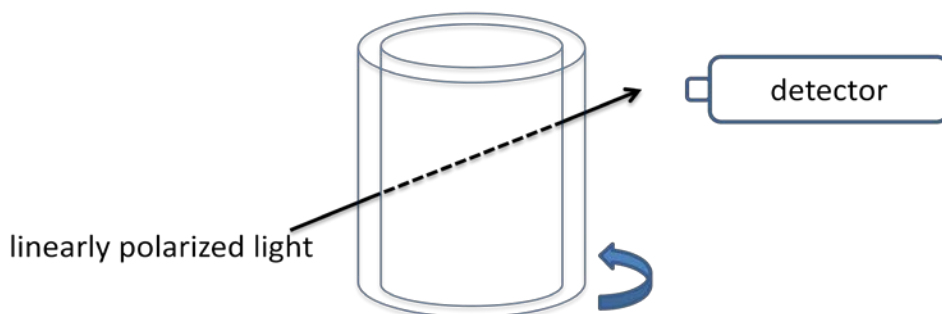


Figure 5 The design of coquette cell. The outer cylinder rotates while the inner cylinder is kept static resulting in a shear flow at the gap between. Liposomes exposed to the deform shear flow and an orientation is gained.

By using this method, the membrane binding orientation of the peptide, either parallel or perpendicular to the membrane surface, can be determined if the membrane binding is in a non-random fashion. The reduced linear dichroism LD^r for liposomes [29] is defined as:

$$LD^r = \frac{LD}{A_{iso}} = \frac{3}{4}S(1 - 3 \cos^2 \beta) \quad (3)$$

S is the membrane orientation factor, which is 1 for full orientation and 0 for random orientation, and β presents the angle between the normal axis of the membrane surface and the orientation of the peptides [28, 31]. Retinal, which aligns almost parallel to the lipid chains in the bilayer [32], can be used as a reference to determine the membrane orientation factor S . Sucrose can be added to reduce light scattering by matching the refractive index of the buffer and increase the viscosity for better liposomes deformation [33]. Since AF16 only absorbs at 225nm (peptide bond absorption at C=O), AF16W and WAF16 were also used in this study to yield a stronger signal. The indole group in tryptophan has three main transition moments, B_b , L_a and L_b [34, 35], shown in Figure 6.

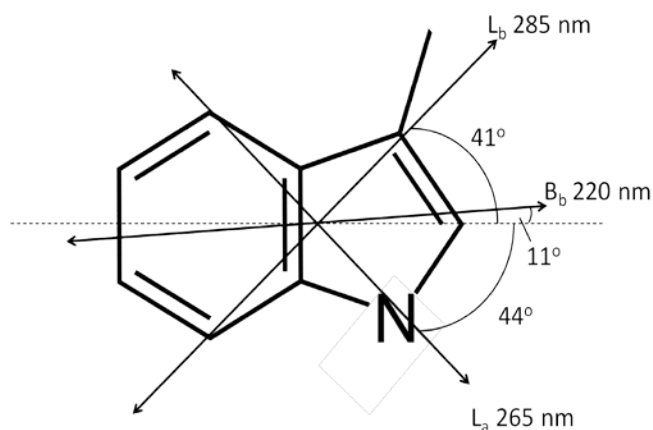


Figure 6 The B_b , L_a and L_b transition moments of indole group in tryptophan which gives LD signal. The dashed line is the pseudosymmetry long axis.

Circular Dichroism (CD) Spectroscopy

Circular Dichroism (CD), which is useful to identify the secondary structure of chiral molecules, is defined as the difference between in absorption of left and right circularly polarized light (Equation (4)) [28, 36].

$$CD = A_l - A_r \quad (4)$$

Electrons rearrangement of chiral molecules under circularly polarized light move in helix, matched with the absorption of circular polarized light, hence the interaction between chiral molecules and left or right circularly polarized light is different [28]. This method can only be used on handed molecules, otherwise absorption in both left in right circularly polarized light are same. The peptide bond has two transition dipole moments which give CD signals, the $n \rightarrow \pi^*$ transition at 220 nm and the $\pi \rightarrow \pi^*$ transition at 190 nm [36]. Since

the CD spectra of different peptide secondary structures have been determined in previous research, the structure of a peptide can be determined by comparing its spectrum with known CD spectra.

Dynamic Light Scattering (DLS)

Particles in solution diffuse under Brownian motion hence fluctuations in the intensity of scattered light can be measured. The autocorrelation of time-dependent fluctuation can be calculated and matched with the diffusion coefficient D . Therefore, the radius of a particle can be calculated by Stokes-Einstein equation [37-39].

Material and Methods

Material

AF16 (VCHSKTRSNPENNVGL) was synthesized by KJ Ross-Petersen ApS (Denmark) and the tryptophan labeled versions were from Innovagen (Sweden). The lipids DOPC (1,2-dioleoyl-sn-glycero-3-phosphocholine), DOPG (1,2-dioleoyl-sn-glycero-3-phosphoglycerol) and DSPE-mPEG2000 (1,2-distearoyl-sn-glycero-3-phosphoethanolamine-N-[methoxy(polyethylene glycol)-2000]) were purchased from Avanti Polar Lipids Inc. and used for preparation of large unilamellar lipid vesicles. ANTS (8-Aminonaphthalene-1,3,6-trisulfonic acid disodium salt) and DPX (p-Xylene-bis(N-pyridinium bromide)), Triton X-100 as well as retinal, were from Sigma Aldrich. The buffer salts and sucrose were also from Sigma Aldrich.

Preparation of Large Unilamellar Vesicles (LUV)

Lipids dissolved in chloroform were mixed in round flask with desired molar ratio. The sample was then dried by rotary evaporator under low vacuum to form a lipids film on the wall of round flask. Final traces of organic solvent were removed under high vacuum for 2 hours. Then the lipid film was dispersed in buffer with a vortex to form liposomes. The choice of buffer depended on the desired pH and requirement of different experiments. After 5 cycles of freezing and thawing [40], liposomes were extruded 21 times through two 100 nm polycarbonate filters with a hand-held extrusion device (LiposoFast, Avestin) [41].

Isothermal Titration Calorimetry (ITC)

Liposomes used in these experiments consisted of 80% DOPC, 15% DOPG and 5% DSPE-mPEG2000. They were suspended in buffer with desired pH, pH7.4 [Na-phosphate 10 mM, NaCl 150 mM, pH7.4] or pH5 [Citrate-phosphate 10 mM, NaCl 150 mM, pH5]. Before experiments, the liposome solution was dialyzed by using a dialysis device (Float-A-Lyzer G2 0.5-1.0 kD, Spectrum Labs) for 3 times, 2 hours each. AF16 was dissolved in dialyzed buffer to minimize the thermal effect during titration. The ITC measurement was carried out using iTC200 MicroCalorimeter from GE Healthcare. 250 μ l of liposomes suspension

was loaded in the reaction cell. 36 μl of AF16 was filled into the syringe and injected into the reaction cell in 0.75-6.00 μl step size with 90-240 sec intervals. Due to dilution of the peptide solution in the syringe needle during thermal equilibration, the volume and concentration of first injection is not accurate. Therefore, the data of first injection was discarded [42]. The heat signal was recorded as a function of time and analyzed by ORIGIN software provided with the instrument.

ANTS/DPX Leakage Assay

The lipid film was dispersed in HEPES buffer containing ANTS and DPX [12.5 mM ANTS, 45 mM DPX, 10 mM HEPES]. The extruded liposomes were separated from the unencapsulated material in a 1.45 x 5.0cm PD-10 buffer exchange column (GE Healthcare) with an elution buffer with desired pH, pH 7.4 [HEPES 10 mM, NaCl 73 mM, pH 7.4] or pH 5 [Citrate-phosphate 10 mM, NaCl 47 mM, pH 5]. The concentration of eluted liposomes was determined by a static light scattering technique, i.e., the intensity of 600 nm light scattered from liposomes was measured and compared with the scattering from liposomes before the buffer exchange. Then liposomes were diluted to lipid concentration 25 μM in 1.5 ml quartz cuvettes with stirring. The fluorescence measurement was performed with Cary Eclipse Fluorescence Spectrophotometer (Agilent Technologies, USA) using an excitation wavelength of 353 nm with 10 nm bandwidth slit and an emission wavelength of 526 nm with 10 nm bandwidth slit. The fluorescence intensities were recorded as a function of time with 10 sec intervals. The content leakage at the beginning was normalized to zero. After 150 sec, the 0.05-0.5 μM AF16 or melittin was added. Melittin is a peptide known to induce pores in liposomes used for contrasting the effect of AF16. The intensity of full leakage was obtained by adding 10 μl 10% Triton X-100. Liposomes contained 20%, 10% or 5% negatively charged lipids, controlled by the mixing ratio of DOPC and DOPG.

Linear Dichroism (LD) Spectroscopy

LD experiments were performed under the follow condition. Lipids, peptides and retinal concentrations were 2.4 mM, 24 μM and 6 μM respectively. 50% sucrose by weight was used in the buffer, pH 7.4 [Na-phosphate 10 mM, NaCl 150 mM, pH 7.4] or pH 5 [Citrate-phosphate 10 mM, NaCl 150 mM, pH5]. LD measurements between 200-500 nm were made on Chirascan Circular Dichroism Spectrometer fitted with a Linear Dichroism Detector (Applied Photophysics, UK). Slit size was 1 nm. Integration time was 0.2 sec. Spectra were accumulated for 10 times and averaged. The shear G inside the coquette cell was 1047 s^{-1} . Baselines were obtained by measuring the LD of reference sample which only contained buffer and liposome. Isotropic absorption spectra were measured with a Varian Cary Bio 50 (Agilent Technologies, USA) using a 1 mm quartz cuvette. Liposomes consisted of 80% DOPC and 20% DOPG.

Circular Dichroism (CD) Spectroscopy

AF16 solution was dissolved in buffer, pH 7.4 [Na-phosphate 10 mM, NaF 150 mM, pH 7.4] or pH 5 [Citrate-phosphate 10 mM, NaF 150 mM, pH 5]. NaF was used instead of NaCl to minimize absorption in UV-region. Samples were placed in a 1 mm quartz cuvette. CD measurements between 180-300 nm were performed on Chirascan Circular Dichroism Spectrometer (Applied Photophysics, UK). Slit size was 2 nm. Integration time was 1 sec. 10 scans were accumulated and averaged. Signals were subtracted by a blank solution to correct background contributions.

Dynamic Light Scattering (DLS)

Measurements were performed on Zetasizer Nano (Malvern Instruments Ltd, UK) at 37.0 °C. Refractive index n was set to 1.570 for both liposomes and AF16 solution.

Fluorescence Spectroscopy

The fluorescence spectra of AF16W and WAF16 were measured between 300-450 nm were measured on a Spex Fluorolog τ -3 spectrofluorometer (JY Horiba). Samples were excited with 280 nm light. Slits were set to 3 or 5 nm depending on the intensity of the sample. Integration time was 0.5 sec. 1 ml of 1 μ M AF16W was loaded in the cuvette and titrated with a 20 mM liposome solution. In each titration, 5 μ l of liposome solution was added and the spectrum was recorded. The fluorescence spectra were corrected for the dilution and background contributions. The buffer used in this experiment were at pH 7.4 [Na-phosphate 10 mM, NaCl 150 mM, pH 7.4] and pH 5 [Citrate-phosphate 10 mM, NaCl 150 mM, pH 5]. Liposomes were composed by 80% DOPC, 15% DOPG and 5% DSPE-mPEG2000.

Results and Discussion

Isothermal Titration Calorimetry (ITC)

When trying to study the binding affinity of AF16 to lipid membranes with ITC, results that were hard to explain were obtained. Variation of peptide concentration did result in unexpected behaviors of the heat flow. In Figure 7, the heat flow of AF16, in a very high concentration, titrated into buffer at pH 7.4 is seen. The maximum heat absorption was observed at the first titration then the heat absorption decreased with the increased AF16 concentration in the reaction cell. Expected result was that the size of peaks should be smaller and remained constant in area if only dilution effect took place. Thus there must be another process but the dilution. An explanation could be that AF16 aggregates in higher concentration. When high concentrated AF16 was injected into the reaction cell, AF16 concentration became lower than its critical aggregating concentration and form monomers. The endothermic process observed is probably due to the fact that energy is needed to break the formed constructs. The aggregation of AF16 was only observed at pH 7.4 but not pH 5, where titration peaks were negative (Figure 9) in a wide range of

concentration, 0.1-2 mM. This is possible due to the higher charge density of AF16 at pH 5 restricts the aggregation.

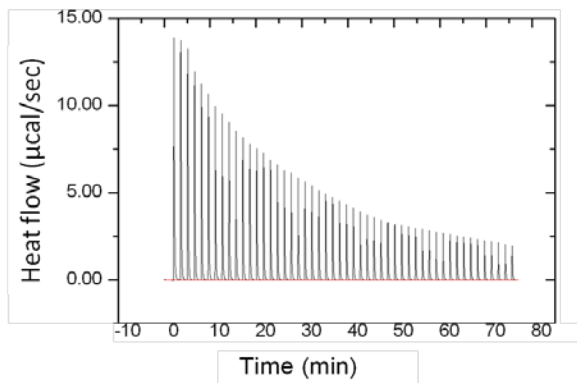


Figure 7 Titration of 32 mM AF16 solution into buffer at pH 7.4.

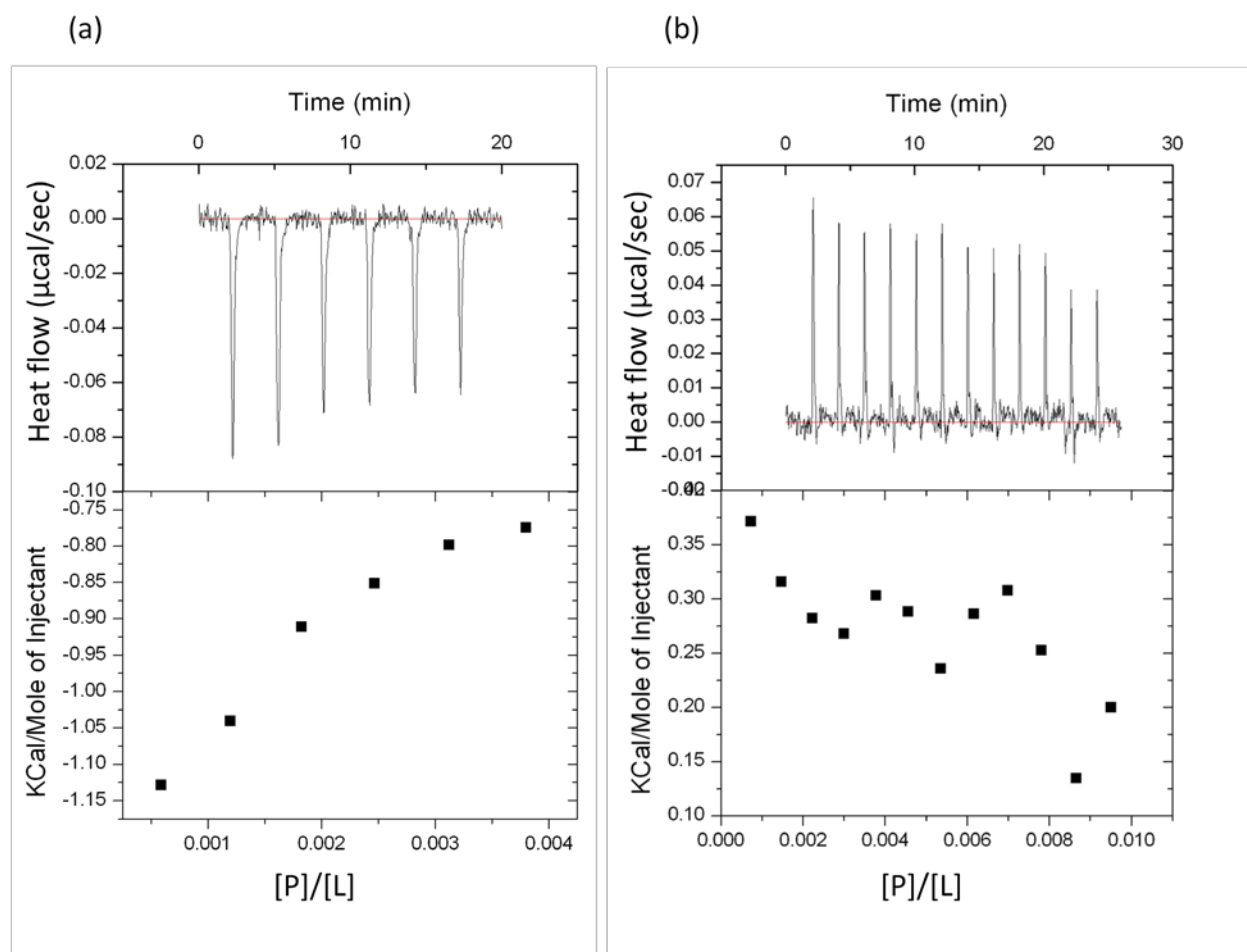


Figure 8 ITC measurements at pH 7.4. 10 mM liposome solutions were titrated with (a) 0.2 mM AF16 and (b) 0.5 mM AF16 solutions. (a) shows negative titration peaks, whereas (b) shows positive peaks.

To determine the aggregating concentration at pH 7.4, AF16 solutions in different concentrations were titrated into 10 mM liposome solutions at pH 7.4. Figure 8 shows the critical point. When 0.5 mM AF16 solution (b) was employed, titration of AF16 was an endothermic process, whereas, a decreased AF16 concentration to 0.2 mM (a) leads to an exothermic process. Therefore, the aggregation point of AF16 is between 0.2 mM and 0.5 mM. The heat absorption due to disaggregation in (b) probably overrides the binding signal but from (a) it is confirmed that the AF16-membrane binding process is an exothermic process. To avoid the disaggregation signal, AF16 concentration should be lower than the concentration where aggregates are found. However, too low concentration leads to undetectable signal for the instrument. One example, 20 mM liposome solution titrated with 0.2 mM AF16 solution at pH 5, is shown in Figure 9. Although the feature of titration peaks was observed, the signal to noise ratio was far from enough for analysis.

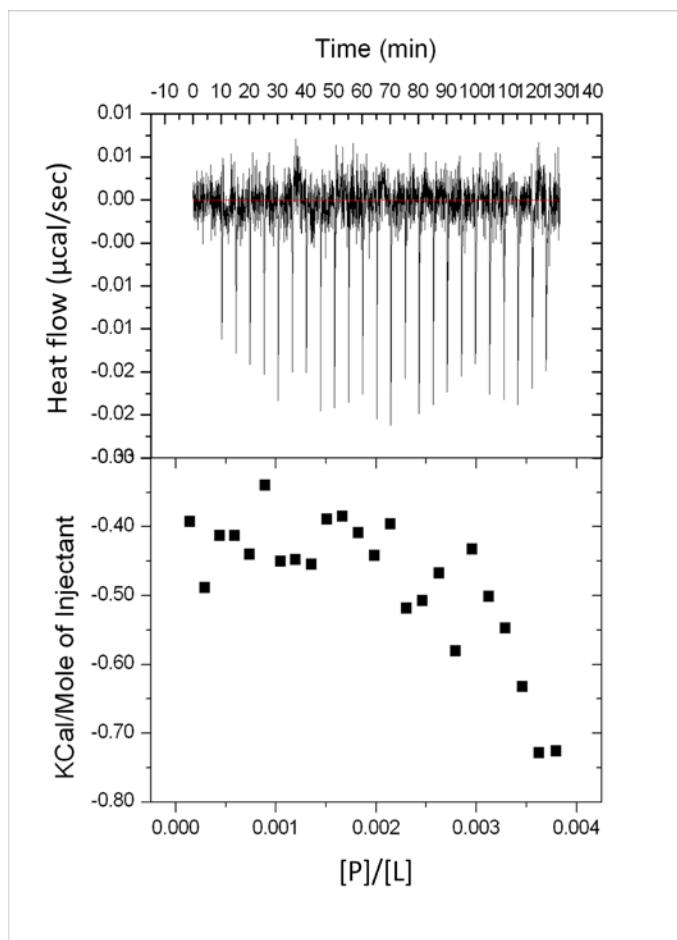


Figure 9 ITC measurements at pH 5. 20 mM liposome solution was titrated with 0.2 mM AF16 solution. The signal to noise ratio was too small.

Dynamic Light Scattering (DLS)

A typical distribution of liposomes size (diameter d) at pH 7.4, 1mM lipid concentration, 37.0 °C is shown in Figure 10. The head group area of DOPC is 0.722 nm² [43] and the length of tails is assumed to be 5 nm. Therefore, one liposome roughly contains 10⁵ lipids.

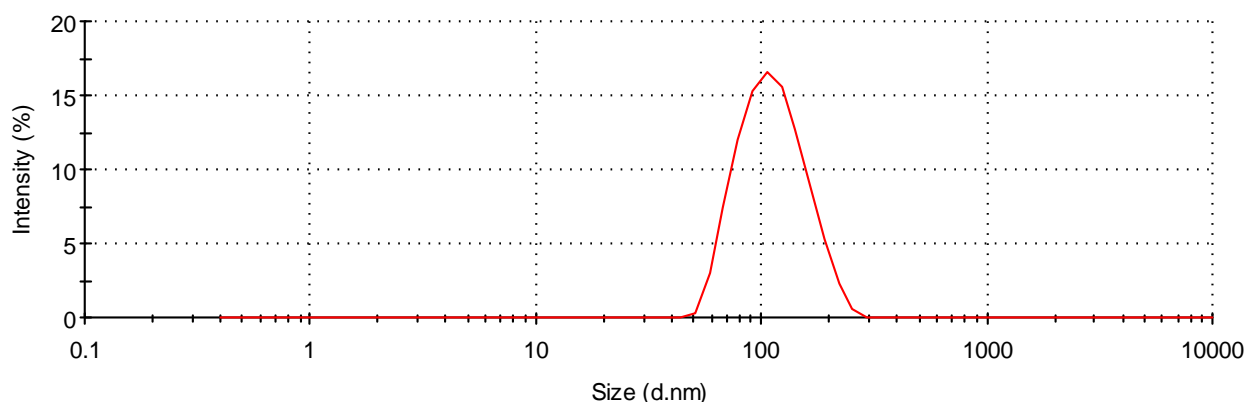


Figure 10 The size (diameter) distribution of liposomes used in experiments. The peak appeared at 116.2 nm.

To study the aggregation of AF16 discovered in ITC measurement, size distributions of AF16 in different concentrations were measurement by DLS. Figure 11 shows the results of 0.2 mM and 1 mM AF16 solution at pH 7.4. The size distribution of concentrated AF16 solution has larger diameter distribution comparing with the lower concentration one which indicates that in high concentration, AF16 aggregates and form larger complex. The aggregation of AF16 is confirmed. However, the refractive index n used in the measurements is for liposomes because this property of the peptide is not known and since the diameter is proportional to n^2 , no absolute or relative size can be determined.

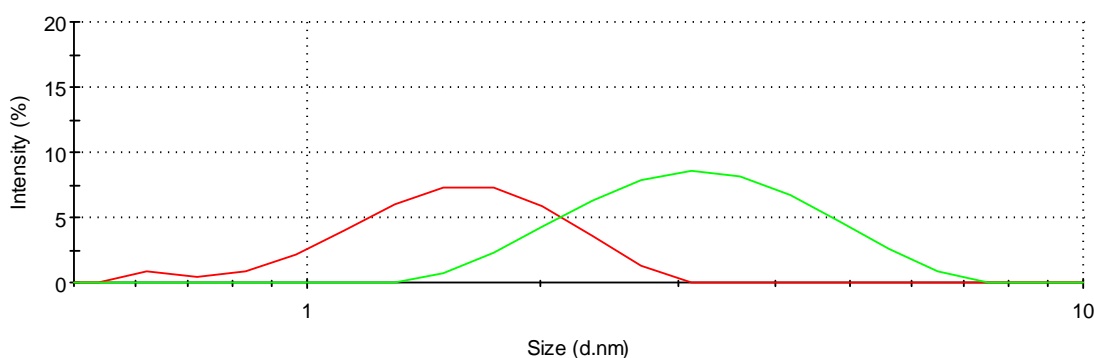


Figure 11 Size (diameter) distributions of AF16 at pH 7.4 in different concentrations: 0.2 mM (red) and 1 mM (green).

Circular Dichroism (CD) Spectroscopy

A series of AF16 CD measurements were performed under different concentrations. Results of using 50 μM AF16 are shown in Figure 12 and compared with previous research [36]. Unbounded AF16 in solution is unstructured at both (a) pH 5 and (b) pH 7.4. Measurement of concentrated AF16 (>0.5 mM) solutions were also performed but high absorption at region <230 nm resulted in unreliable CD spectra. Hence, AF16 aggregation cannot be determined in CD measurements. The CD spectrum of AF16 mixed with liposomes (not shown) is also similar to unbound spectra which indicate that AF16 is also unstructured in membrane bound state.

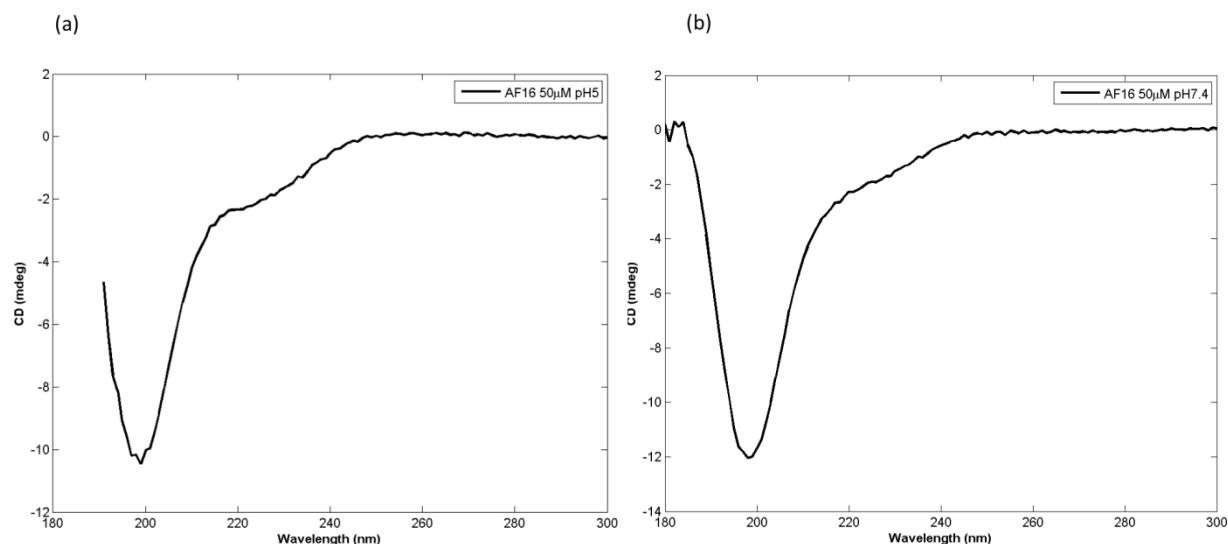


Figure 12 CD spectra of AF16 at (a) pH 5 and (b) pH 7.4 show that AF16 is unstructured in solution. The dashed line at (a) indicates that the spectrum not reliable at region <190 nm.

ANTS/DPX Leakage Assay

To confirm that AF16 does not cause pore formation in lipid membranes, ANTS/DPX leakage assay was employed. In each experiment, three samples ran in parallel, corresponded to addition of AF16, melittin and the control setup (reference, no peptide addition). Melittin is a peptide which is known to induce pores in liposomes and was used for contrasting the effect of AF16. One leakage experiment at pH 5 is shown in Figure 13. ANTS leaked from liposomes was recorded with time. In this experiment, peptides in concentration 0.1 μM were added at the time 150 sec. However, some leakage (2.5%) was observed already before the addition of peptides, which could be due to a difference in osmotic pressure between elution buffer and encapsulated buffer. After the addition of peptides, the liposomes which interacting with melittin leaked 20% of content in 50 sec, whereas the content leakage in AF16 addition sample and control sample remained steady.

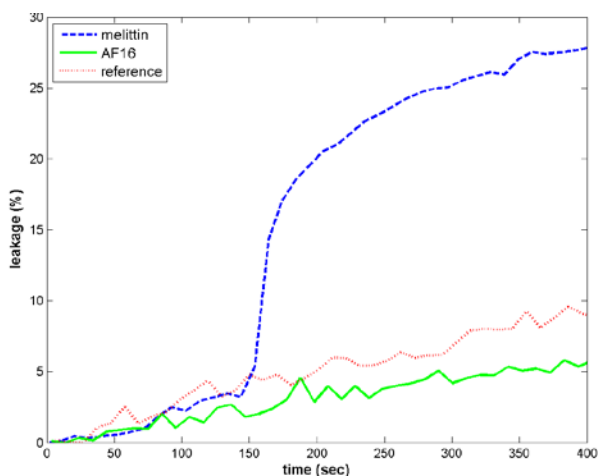


Figure 13 The leakage experiment of 10% negative charge liposomes at pH 5. Peptides were added up to 0.1 μM at 150 sec.

Experiments were done under different conditions: pH 5 and pH 7.4; liposomes containing 20%, 10% and 0% negatively charged lipids; and concentrations of 0.05 μM , 0.1 μM and 0.5 μM of the peptides. Typical results, where high peptide concentration (0.5 μM) was employed, are shown in Figure 14 (a) and (b) corresponding to conditions at pH 5 and pH 7.4. There were no leakage effects after addition of AF16 at the time 125 sec. Moreover, experiments under other conditions also show the same result. Thus, AF16 does not cause contents leakage of ANTS upon binding to lipid membranes. Since the membrane-AF16 interaction is not strong in the ITC measurements, the result is reasonable.

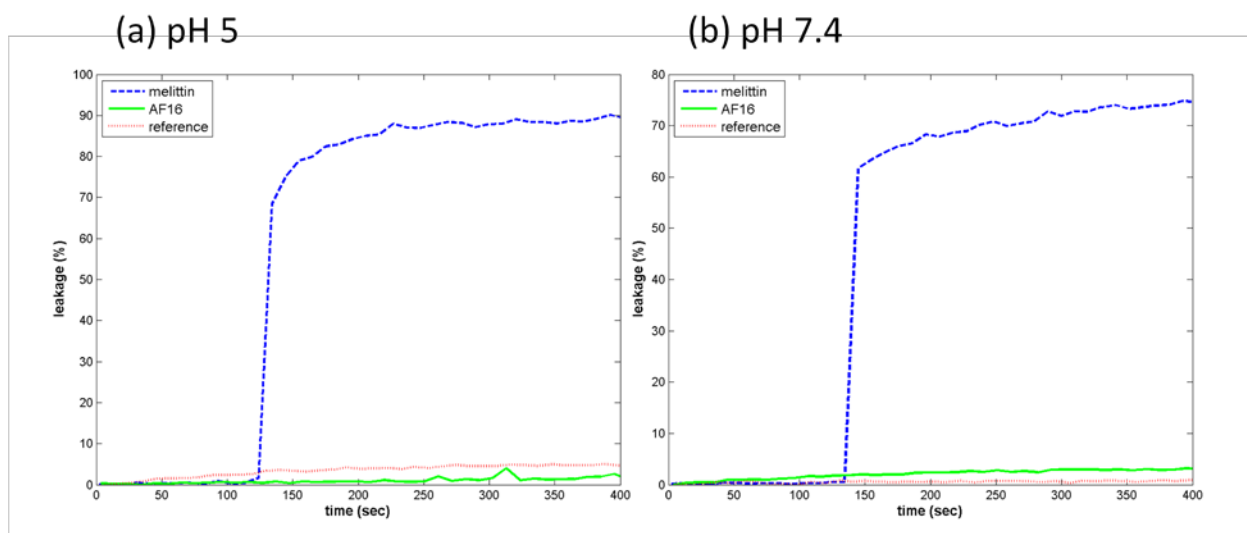


Figure 14 Leakage experiments of 20% negative charge liposomes at (a) pH 5 and (b) pH 7.4. Lipid and peptides concentration were 25 μM and 0.5 μM . Peptides were added at the time about 125 sec. Both results show that AF16 did not cause contents leakage.

Linear Dichroism (LD) Spectroscopy

Figure 15 (a) and (b) show the LD and LD^r spectrum of AF16, AF16W or WAF16 and retinal in the presence of liposomes at pH 5. Negative peaks at 391 nm in the LD spectrum correspond to the retinal, which inserted into the membrane almost perpendicular to the surface. The dip in the AF16 LD spectrum at 226 nm indicates the $n \rightarrow \pi^*$ transition of peptide bond amide chromophore which means that AF16 binds to lipid membrane. In the LD^r spectrum, dips at 226 nm in AF16W and WAF16 spectra are more significant than in AF16 spectrum. This could be due to two possible reasons. Firstly, since the labeling tryptophan is a hydrophobic amino acid and contains an indole functional group, the peptide membrane binding become stronger. Secondly, tryptophan has a LD transition moment at 220 nm [28] and this signal overlaps with the 226 nm dip which means that the B_b transition of the tryptophan is aligned with the lipid chains. However, it is hard to tell how the rest of the amino acids are. Other transition moments, L_a and L_b, from tryptophan are not clear in the LD spectrum because they are weaker than B_b. The tilting between 250-300 nm in the LD^r spectra is due to the existing of retinal, proved from separated LD experiments of sample without retinal. The insertion angle of retinal is 35° [32] hence the orientation factor S calculated by Equation (3) is 0.0099. Both the shear G and S in this system are three times smaller than previous research on retinal.

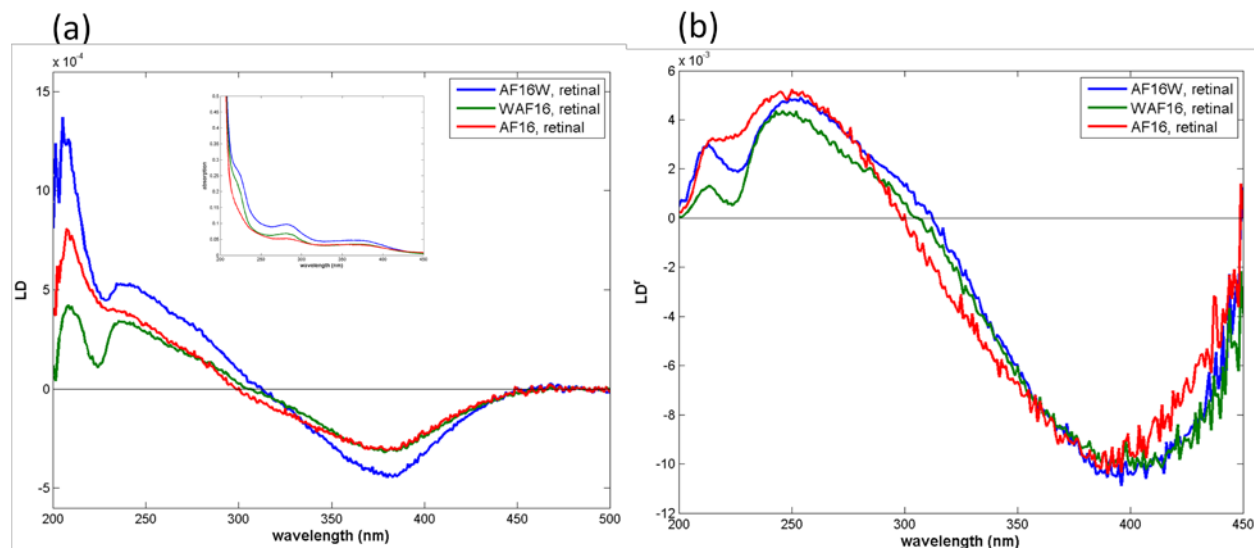


Figure 15 (a) LD spectra inserted absorption spectra and (b) LD^r spectra of the peptides and retinal at pH 5.

LD and LD^r spectra measurements were also performed at pH 7.4 and are shown in Figure 16. The LD^r spectrum shows that the retinal orientation was affected by the presence of the tryptophan because in AF16W and WAF16 spectra, the LD^r values at 380 nm are less negative.

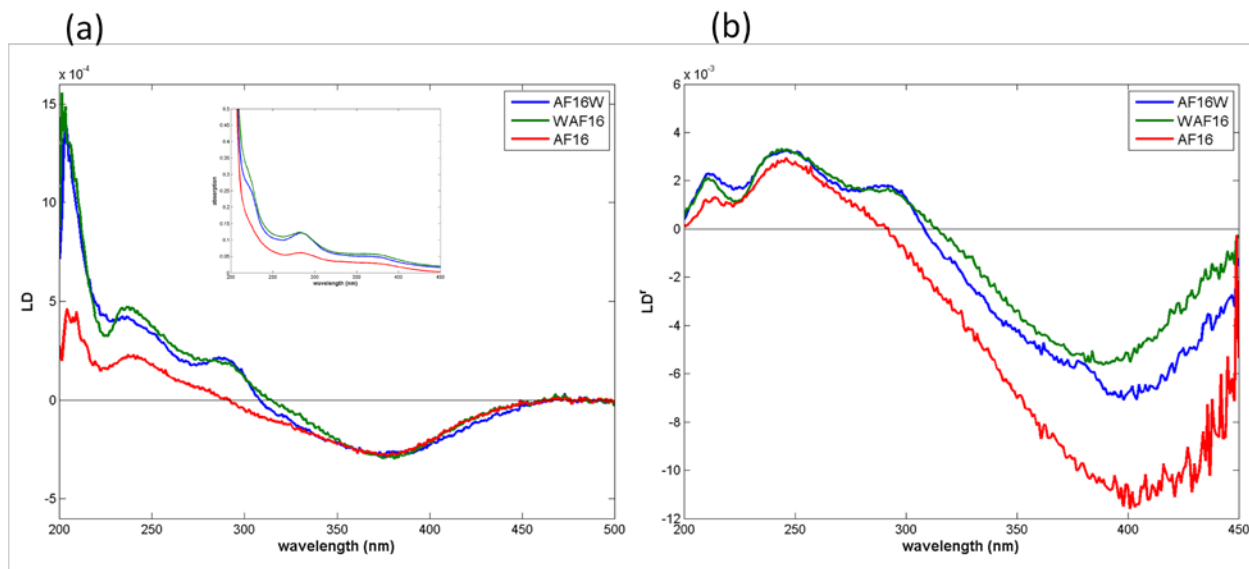


Figure 16 LD (a) spectra with inserted absorption spectra and LD' (b) spectra of the peptides and retinal at pH 7.4.

Fluorescence Spectroscopy

Colored curves in Figure 17 show the fluorescence spectra during stepwise titration of liposomes into AF16W solution (the arrow indicates addition direction) at pH 5. The lower dashed curve refers to the reference spectrum of peptide free in solution, whereas the upper dashed curve is the reference spectrum of membrane-bound peptide where concentration of lipids was 150% of last titration step, and it was assumed that all peptides bound to liposomes due to the high concentration of lipids. Since the peptide was found to absorb to the cuvette and pipet tips, the reference for membrane bound peptide was done in a separated experiment. In aqueous buffer, the fluorescence maximum is at 354 nm. After addition of liposomes, more and more peptides bind to the lipid membranes, resulting in the blue shift and increased fluorescence intensity. This is due to that tryptophan emission has higher quantum yield and becomes blue shifted when transferring from polar environment to less polar environment [18]. The spectrum of fully membrane-bound peptide has the maximum fluorescence at 330 nm. The shift is larger comparing with pervious researches, 10-12 nm [19, 20], hence the indole group seems to be more shielded from the aqueous solution. The quantum yield of membrane-bound state is 2.8 times higher than the one for the free peptide.

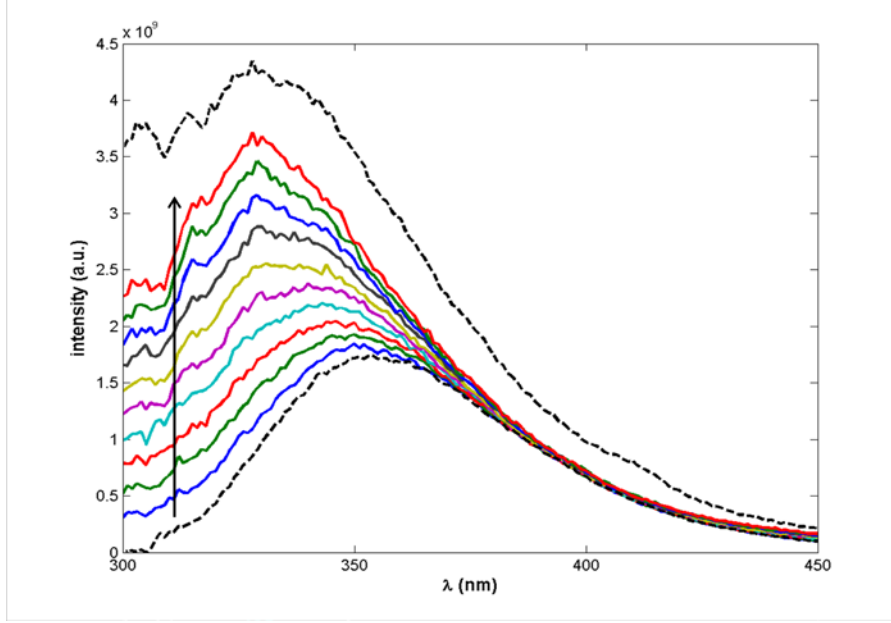


Figure 17 Fluorescence spectra of titration AF16W with liposomes solution at pH 5 (increasing liposome concentration is indicated by the arrow in the figure). Dashed curve are the reference spectrum of fully free peptide (lower trace) and fully bounded peptide (upper trace) collected in separated experiment.

The concentrations of peptide free in solution $[P_f]$ and membrane-bound peptide $[P_b]$ were analyzed with singular value decomposition (SVD). The spectra data were collected as columns in a matrix D . This matrix is decomposed by SVD:

$$D = USV^T \quad (5)$$

The first three columns of U were plotted in Figure 18. Only the first two columns have non-random structure. This consists that those fluorescence spectra in Figure 17 are only due to two species, free and bound state of the peptide. The jump at around 10 nm in the third column is probably due to the Raman peak from water. Since the system only contains two species,

$$D \approx RC^T \quad (6)$$

where R is the matrix of two reference spectra (first column refers to the free peptide spectrum and second column refers to the membrane-bound peptide spectrum). C is a two columns matrix, where the first column is the free peptide concentration $[P_f]$ and the second column is the membrane-bound peptide concentration $[P_b]$ in different titration step, which can be calculated by

$$C^T = (R^T R)^{-1} R^T D \quad (7)$$

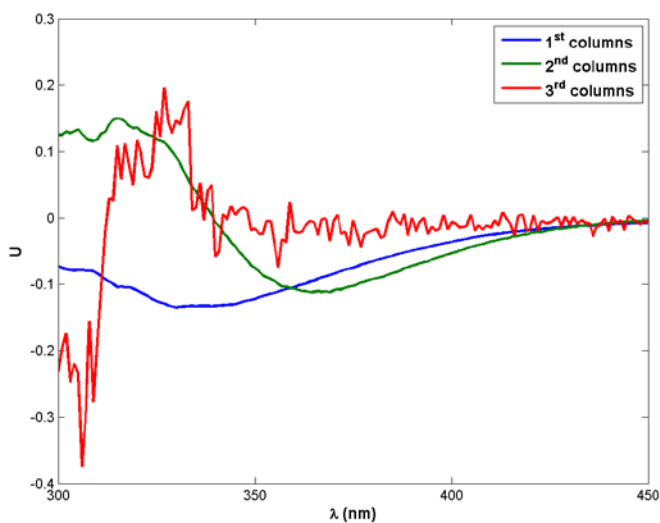


Figure 18 The first three columns of U . Since only the first two columns have non-random structure, they are enough for describing titration spectra in Figure 17. The rest are only noise. The relative singular values are 1, 0.1455 and 0.0053.

The binding isotherm of AF16W to liposomes at pH 5 is shown in Figure 19. Less than 50% of AF16W bound to liposomes when the peptide to lipid ratio $[P]:[L]$ is higher than 1:2674 which indicates that the binding is weak.. It is therefore likely that the assumption that the reference spectra for fully bound peptide is containing some free peptide as well. It is also important to remember that the peptide used in this experiment was labeled with tryptophan, which affects the peptide binding properties. Since tryptophan is highly hydrophobic, AF16 is possible an even weaker binder to liposomes. The concentration of peptide at the last titration step was $0.8084 \mu\text{M}$ which means 20% of peptide was lost during titration process, since the initial peptide concentration was $1 \mu\text{M}$.

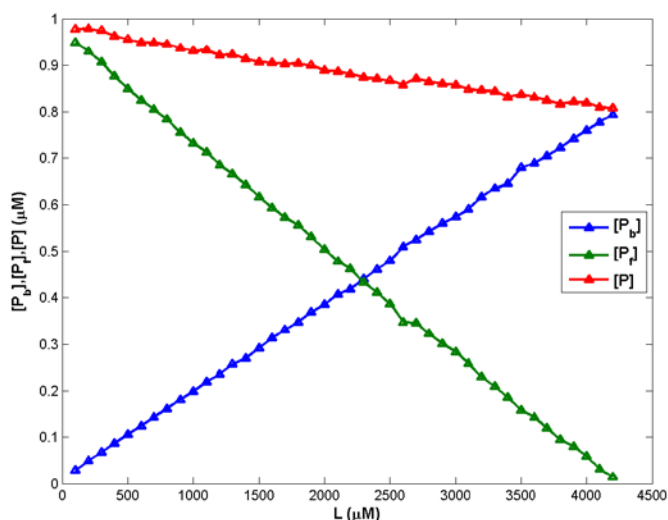


Figure 19 Binding isotherm of AF16W to liposomes at pH 5. Less than 50% of AF16W bind to liposomes when the peptide to lipid ratio $[P]:[L]$ is higher than 1:2674.

Similar experiment was repeated at pH 7.4, with different settings. However, in this case the spectra did not saturate in intensity. The reference spectrum of membrane-bound peptide was recorded at peptide to liposome ratio equal to 1:1, assumed that all peptides bound to liposomes due to the high concentration of lipids. The binding isothermal is shown in Figure 20. At pH 7.4, 50% binding occurred at $[P]:[L]=1:14117$ which means the binding is much weaker comparing with at pH 5. This result agrees with the expectation since the peptide is more positively charged at pH 5 and likely to bind to negatively charged membrane.

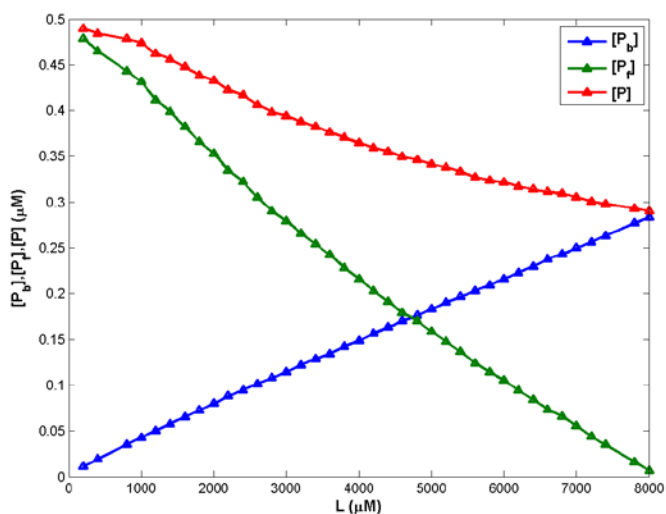


Figure 20 Binding isotherm of AF16W to liposomes at pH 7.4. Less than 50% of AF16W bind to liposomes when the peptide to lipid ratio $[P]:[L]$ is higher than 1:14117.

Concluding Remarks

A series of methods was used to study the AF16-membrane interaction and results are concluded in this section. From the LD spectrum, binding of AF16 to membrane is observed though the binding geometry is not confirmed. From the fluorescence spectrum result, AF16W is more likely to bind to membrane at pH 5, however, the binding seems to be very weak at both pH 5 and pH 7.4. It is likely that the peptide does not interact with lipids but rather with proteins or gangliosides on real cells. ANTS/DPX assay shows AF16 does not cause ANTS leakage at both pH 5 and pH 7.4 hence AF16 does not cause pore formation in lipid bilayers. It is not possible to determine the binding affinity with the use of ITC, it was concluded, with the support of DLS, that AF16 aggregation occurs between 0.2-0.5 mM at pH 7.4. Thus, high concentration AF16 should be avoided in experiments unless the aggregation state is of interest.

Future Aspect

Since binding affinity seems to be hard to determine in these conditions using ITC and fluorescence spectroscopy, other techniques could be employed. Surface sensitive techniques, surface plasma resonance (SPR) and quartz crystal microbalance (QCM), can be alternative methods. It could also be of interest to try other lipids in the liposomes or liposomes with membrane proteins to see if the affinity can be increased.

Regarding the leakage experiment, it is important to notice that leakage of ANTS can only occur through pores larger than around 1 nm due to the molecular size. Therefore, ANTS/DPX assay can only investigate if there are pores larger than 1 nm on lipid membrane. The choice of using these large molecules are i) ANTS can be detected by fluorescence technique; ii) the dynamic motion of lipid bilayer in liposomes can induce small pore resulting in very small molecules penetrate through the bilayer. Therefore, it is difficult to select a molecule with suitable size for leakage assay. Recently, SPR has been used for determining permeability of molecule across the lipid membrane [44]. Under passive diffusion, the permeability of molecule across the membrane is related to the amount of pores which are larger or have comparable size formed on the lipid membrane. Therefore, comparing the permeability of small molecule, e.g. xylitol or even Ca^+ ion, in peptide existing environment with control setup could be a solution of determining if peptide induces pores formation.

Acknowledgement

I would like to thank the following people:

Stefan Lange, Ivar Lönnroth, Eva Janniche and Ewa Johansson from Gothenburg University – Thanks for providing us the peptides we used in this thesis and also a project idea.

Bengt Nordén – Thanks for the comment and suggestion on my thesis.

Per Lincoln – Thanks for the discussion on tryptophan emission spectra.

My supervisor, Maria Matson Dzebo – Thanks for the great support and guild.

My parents and brother – Thanks for your encouragement.

References

1. UNICEF and WHO, *Diarrhoea: Why children are still dying and what can be done*. 2009.
2. Lönnroth, I., S. Lange, and E. Skadhauge, *The antisecretory factors: Inducible proteins which modulate secretion in the small intestine*. *Comparative Biochemistry and Physiology Part A: Physiology*, 1988. **90**(4): p. 611-617.
3. Lönnroth, I. and S. Lange, *Purification and characterization of the antisecretory factor: a protein in the central nervous system and in the gut which inhibits intestinal hypersecretion induced by cholera toxin*. *Biochimica et Biophysica Acta (BBA) - General Subjects*, 1986. **883**(1): p. 138-144.
4. Johansson, E., et al., *Molecular-cloning and Expression of a Pituitary-gland Protein Modulating Intestinal Fluid Secretion*. *Journal of Biological Chemistry*, 1995. **270**(35): p. 20615-20620.
5. Johansson, E., S. Lange, and I. Lönnroth, *Identification of an active site in the antisecretory factor protein*. *Biochimica et Biophysica Acta (BBA) - Molecular Basis of Disease*, 1997. **1362**(2-3): p. 177-182.
6. Jennische, E., et al., *The peptide AF-16 abolishes sickness and death at experimental encephalitis by reducing increase of intracranial pressure*. *Brain Research*, 2008. **1227**(0): p. 189-197.
7. Johansson, E., et al., *Antisecretory factor suppresses intestinal inflammation and hypersecretion*. *Gut*, 1997. **41**(5): p. 642-642.
8. Lange, S. and I. Lönnroth, *The antisecretory factor: Synthesis, anatomical and cellular distribution, and biological action in experimental and clinical studies*, in *International Review of Cytology*, W.J. Kwang, Editor. 2001, Academic Press. p. 39-75.
9. Eriksson, A., et al., *Effect of antisecretory factor in ulcerative colitis on histological and laborative outcome: a short period clinical trial*. *Scandinavian Journal of Gastroenterology*, 2003. **38**(10): p. 1045-1049.

10. Björck, S., et al., *Food induced stimulation of the antiseecretory factor can improve symptoms in human inflammatory bowel disease: a study of a concept*. Gut, 2000. **46**(6): p. 824-829.
11. Lange, S., et al., *Food-induced antiseecretory factor activity is correlated with small bowel length in patients with intestinal resections*. APMIS, 2003. **111**(10): p. 985-988.
12. Hanner, P., et al., *Increased antiseecretory factor reduces vertigo in patients with Ménière's disease: a pilot study*. Hearing Research, 2004. **190**(1-2): p. 31-36.
13. Zaman, S., et al., *B 221, a medical food containing antiseecretory factor reduces child diarrhoea: a placebo controlled trial*. Acta Pædiatrica, 2007. **96**(11): p. 1655-1659.
14. Lönnroth, I., et al., *Cholera toxin protects against action by Clostridium difficile toxin A*. APMIS, 2003. **111**(10): p. 969-977.
15. Campbell, M.K. and S.O. Farrell, *Biochemistry*. 2011: BROOKS COLE Publishing Company.
16. Rapallino, M.V., et al., *Antiseecretory factor peptide derivatives specifically inhibit [3H]- γ -amino-butyric acid/ $^{36}\text{Cl}^-$ out \rightarrow in permeation across the isolated rabbit Deiters' neuronal membrane*. Acta Physiologica Scandinavica, 2003. **179**(4): p. 367-371.
17. Bowen, E.J., *Fluorescence and fluorescence quenching*. Quarterly Reviews, Chemical Society, 1947. **1**(1): p. 1-15.
18. Vivian, J.T. and P.R. Callis, *Mechanisms of Tryptophan Fluorescence Shifts in Proteins*. Biophysical Journal, 2001. **80**(5): p. 2093-2109.
19. Persson, D., et al., *Application of a Novel Analysis To Measure the Binding of the Membrane-Translocating Peptide Penetratin to Negatively Charged Liposomes†*. Biochemistry, 2002. **42**(2): p. 421-429.
20. Caesar, C.E.B., et al., *Membrane Interactions of Cell-Penetrating Peptides Probed by Tryptophan Fluorescence and Dichroism Techniques: Correlations of Structure to Cellular Uptake†*. Biochemistry, 2006. **45**(24): p. 7682-7692.
21. Esbjörner, E.K., et al., *Tryptophan orientation in model lipid membranes*. Biochemical and Biophysical Research Communications, 2007. **361**(3): p. 645-650.
22. Ellens, H., J. Bentz, and F.C. Szoka, *pH-Induced destabilization of phosphatidylethanolamine-containing liposomes: role of bilayer contact*. Biochemistry, 1984. **23**(7): p. 1532-1538.

23. Epand, R.F., et al., *Direct comparison of membrane interactions of model peptides composed of only Leu and Lys residues*. Peptide Science, 2003. **71**(1): p. 2-16.
24. Guo, X., J.A. MacKay, and F.C. Szoka, Jr., *Mechanism of pH-triggered collapse of phosphatidylethanolamine liposomes stabilized by an ortho ester polyethyleneglycol lipid*. Biophysical Journal, 2003. **84**(3): p. 1784-95.
25. Düzgüneş, N., H. Faneca, and M.P. Lima, *Methods to Monitor Liposome Fusion, Permeability, and Interaction with Cells*, in *Liposomes*, V. Weissig, Editor. 2010, Humana Press. p. 209-232.
26. Freire, E., O.L. Mayorga, and M. Straume, *Isothermal titration calorimetry*. Analytical Chemistry, 1990. **62**(18): p. 950A-959A.
27. Leavitt, S. and E. Freire, *Direct measurement of protein binding energetics by isothermal titration calorimetry*. Current Opinion in Structural Biology, 2001. **11**(5): p. 560-566.
28. Nordén, B., A. Rodger, and T. Dafforn, *Linear Dichroism and Circular Dichroism: A Textbook on Polarized-Light Spectroscopy*. 2010, London: The Royal Society of Chemistry. 293.
29. Rodger, A., et al., *Flow oriented linear dichroism to probe protein orientation in membrane environments*. Physical Chemistry Chemical Physics, 2002. **4**(16): p. 4051-4057.
30. Ardhammar, M., N. Mikati, and B. Nordén, *Chromophore Orientation in Liposome Membranes Probed with Flow Dichroism*. Journal of the American Chemical Society, 1998. **120**(38): p. 9957-9958.
31. Matson, M., et al., *Spectral Properties and Orientation of Voltage-Sensitive Dyes in Lipid Membranes*. Langmuir, 2012. **28**(29): p. 10808-10817.
32. Svensson, F.R., et al., *Retinoid Chromophores as Probes of Membrane Lipid Order*. The Journal of Physical Chemistry B, 2007. **111**(36): p. 10839-10848.
33. Ardhammar, M., P. Lincoln, and B. Nordén, *Invisible liposomes: Refractive index matching with sucrose enables flow dichroism assessment of peptide orientation in lipid vesicle membrane*. Proceedings of the National Academy of Sciences, 2002. **99**(24): p. 15313-15317.
34. Albinsson, B. and B. Norden, *Excited-state properties of the indole chromophore: electronic transition moment directions from linear dichroism measurements: effect of methyl and methoxy substituents*. The Journal of Physical Chemistry, 1992. **96**(15): p. 6204-6212.
35. Albinsson, B., et al., *Near-ultraviolet electronic transitions of the tryptophan chromophore: linear dichroism, fluorescence anisotropy, and*

- magnetic circular dichroism spectra of some indole derivatives*. The Journal of Physical Chemistry, 1989. **93**(18): p. 6646-6654.
36. Kelly, S.M. and N.C. Price, *Circular Dichroism: Studies of Proteins*, in *eLS*. 2001, John Wiley & Sons, Ltd.
 37. Kaszuba, M., et al., *Resolving Concentrated Particle Size Mixtures Using Dynamic Light Scattering*. Particle & Particle Systems Characterization, 2007. **24**(3): p. 159-162.
 38. Hupfeld, S., et al., *Liposome Size Analysis by Dynamic/Static Light Scattering upon Size Exclusion-/Field Flow-Fractionation*. Journal of Nanoscience and Nanotechnology, 2006. **6**(9-10): p. 3025-3031.
 39. Tscharnuter, W., *Photon Correlation Spectroscopy in Particle Sizing*, in *Encyclopedia of Analytical Chemistry*. 2006, John Wiley & Sons, Ltd.
 40. Monnard, P.-A., T. Oberholzer, and P. Luisi, *Entrapment of nucleic acids in liposomes*. Biochimica et Biophysica Acta (BBA) - Biomembranes, 1997. **1329**(1): p. 39-50.
 41. Mayer, L.D., M.J. Hope, and P.R. Cullis, *Vesicles of variable sizes produced by a rapid extrusion procedure*. Biochimica et Biophysica Acta (BBA) - Biomembranes, 1986. **858**(1): p. 161-168.
 42. Arouri, A., et al., *Hydrophobic interactions are the driving force for the binding of peptide mimotopes and Staphylococcal protein A to recombinant human IgG1*. European Biophysics Journal, 2007. **36**(6): p. 647-660.
 43. Tristram-Nagle, S., H.I. Petrache, and J.F. Nagle, *Structure and Interactions of Fully Hydrated Dioleoylphosphatidylcholine Bilayers*. Biophysical Journal, 1998. **75**(2): p. 917-925.
 44. Brändén, M., et al., *Refractive-Index-Based Screening of Membrane-Protein-Mediated Transfer across Biological Membranes*. Biophysical Journal, 2010. **99**(1): p. 124-133.